Published in final edited form as:
Cell. 2012 September 14; 150(6): 1264–1273. doi:10.1016/j.cell.2012.08.020.

Long-Distance Growth and Connectivity of Neural Stem Cells After Severe Spinal Cord Injury

Paul Lu[1,2,*], **Yaozhi Wang**[1], **Lori Graham**[1], **Karla McHale**[1], **Mingyong Gao**[1], **Di Wu**[1], **John Brock**[1], **Armin Blesch**[1], **Ephron S. Rosenzweig**[1], **Leif A. Havton**[3], **Binhai Zheng**[1], **James M. Conner**[1], **Martin Marsala**[4], and **Mark H. Tuszynski**[1,2,*]

[1]Dept. of Neurosciences, University of California - San Diego, La Jolla, CA 92093, USA

[2]Veterans Administration Medical Center, San Diego, CA 92161, USA

[3]Dept. of Neurology, University of California, Los Angeles, CA 90095, USA

[4]Dept. of Anesthesiology, University of California, - San Diego, CA 92093, USA

SUMMARY

Neural stem cells (NSCs) expressing GFP were embedded into fibrin matrices containing growth factor cocktails and grafted to sites of severe spinal cord injury. Grafted cells differentiated into multiple cellular phenotypes, including neurons, which extended large numbers of axons over remarkable distances. Extending axons formed abundant synapses with host cells. Axonal growth was partially dependent on mammalian target of rapamycin (mTOR) but not Nogo signaling. Grafted neurons supported formation of electrophysiological relays across sites of complete spinal transection, resulting in functional recovery. Two human stem cell lines (566RSC and HUES7) embedded in growth factor-containing fibrin exhibited similar growth, and 566RSC cells supported functional recovery. Thus, properties intrinsic to early stage neurons can overcome the inhibitory milieu of the injured adult spinal cord to mount remarkable axonal growth resulting in formation of novel relay circuits that significantly improve function. These therapeutic properties extend across stem cell sources and species.

INTRODUCTION

Research over the last several decades has revealed numerous molecular mechanisms in the environment of the adult central nervous system (CNS) that contribute to the failure of axonal regeneration after injury, including myelin-associated proteins that inhibit axonal growth (He and Koprivica, 2004; Buchli and Schwab, 2005), the deposition of inhibitory extracellular matrix molecules around injury sites (Fawcett, 2006; Fitch and Silver, 2008), and the lack of positive environmental stimuli such as growth factors (Tuszynski and Lu, 2008). The observation that at least some classes of adult CNS axons can grow over long distances in peripheral nerve bridges supports the view that the adult CNS environment is inhibitory (David and Aguayo, 1981; Houle et al., 2006). However, some studies indicate that neuron-intrinsic mechanisms also contribute to axonal growth failure in the adult CNS

[*]Correspondence to: Mark H. Tuszynski or Paul Lu, Dept. Neurosciences, 0626 University of California, San Diego, La Jolla, CA 92093, USA 858-534-8857 858-534-5220 (fax) mtuszynski@ucsd.eduplu@ucsd.edu.

The authors declare that they have no competing financial interests.

(Filbin, 2006; Kadoya et al., 2009). Indeed, the extent to which neuron-intrinsic mechanisms alone can overcome the inhibitory growth environment of the adult CNS is actively debated. To address this question, we grafted either freshly dissociated neural stem cells/progenitors from green fluorescent protein (GFP) - expressing rat embryos (Bryda et al., 2006; Baska et al., 2008; Mayer-Proschel et al., 1997), or cultured human stem cells derived from two different sources (HUES7 cells and 566RSC cells from NeuralStem Inc.) to the adult lesioned spinal cord. Expression of the GFP reporter gene in all cells provides an unprecedented opportunity to track the fate, integration, process extension and differentiation of grafted cell types within the inhibitory milieu of the adult injured spinal cord.

We now report a remarkable capability of early stage neurons from different sources and species to survive, integrate, extend axons over very long distances and form functional relays in the lesioned adult CNS. These findings indicate that, despite the inhibitory milieu of the adult CNS, neuron-intrinsic mechanisms are sufficient to support remarkably extensive axonal growth and synapse formation after spinal cord injury, resulting in formation of novel neuronal relays that restore electrophysiological activity and behavior. Moreover, stem cells across species exhibit these properties, supporting the intrinsic capabilities of these cells and suggesting translational relevance.

RESULTS

Fischer 344 adult rats underwent T3 complete spinal cord transection. Two weeks later, a clinically relevant time point, we dissected embryonic day 14 (E14) spinal cords from Fischer 344 rats ubiquitously expressing the GFP reporter gene. Grafts were trypsinized and implanted as suspensions (Giovanini et al., 1997), but survived only at the host/lesion margins and failed to fill the complete transection site. To enhance graft survival and filling of the lesion, in new experiments the E14 neural stem cells were embedded into fibrin/thrombin matrices containing a cocktail of growth factors (N=26 rats; see Methods). Animals then underwent functional and electrophysiogical studies and were perfused 9 weeks after the initial injury.

Anatomical analysis revealed that grafted cells completely and consistently filled the lesion cavity when assessed seven weeks post-grafting (Fig. 1A–1B). Grafted cells were not observed to migrate into the host beyond the immediate region of the graft/lesion site. Grafted cells primarily differentiated into neurons (27.5 ± 2.7% of all GFP-labeled cells), oligodendroglia (26.6 ± 3.9%) and astrocytes (15.9 ± 1.6%) (Fig. 1C–1H and Suppl. Fig. 1). Numerous large GFP-labeled cells co-localized with the mature neuronal markers NeuN (Fig. 1C–1H), βIII tubulin (Tuj1) and MAP2 (Suppl. Fig. 2A–B). In addition to expressing mature neuronal markers, many grafted cells also expressed choline acetyltransferase (ChAT), characteristic of spinal motor neurons, and the inhibitory neuronal marker glutamic acid decarboxylase 67 (GAD67) (Suppl. Fig. 2C–D).

Graft-derived spinal cord neurons extended large numbers of axons into the host spinal cord in both rostral and caudal directions over remarkably long distances (Fig. 2). Emerging GFP-labeled processes from grafts were axons, as demonstrated by co-labeling for the axonal marker neurofilament (Fig. 2A). In the cephalad (rostral) direction, graft-derived axons extended to C6 in all subjects examined (N = 6), and a distance of 25 mm from the T3 transection cavity into the C4 cervical segment in 5 of 6 subjects (Fig. 2E–F). Graft-derived axons also extended caudally to the lower thoracic spinal cord (T10) in all subjects (N = 6), continuing to the upper lumbar spinal cord, a distance of more than nine spinal segments (25 mm), in 4 of 6 subjects (2A–D, G–H). All animals with caudal extension of axons to L1 also exhibited rostral extension of axons to C4, indicating that long-distance, bi-directional

axonal growth occurred commonly. To estimate the magnitude of axon outgrowth that can be achieved by implantation of neural primordia into sites of spinal cord injury, we stereologically (Rosenzweig et al., 2010) quantified 29,000 GFP-labeled axons *emerging* from the graft in the caudal direction (0.5 mm caudal to the T3 transection site). This number likely represents an underestimation, as dense bundles of axons that could not be individually resolved were counted as single axons. The density of axons emerging from grafts was highly consistent among all six subjects examined (Suppl. Fig. 3). In 12 additional subjects, progressive axon emergence from the lesion/graft site was serially examined at time points of 1, 2, 3 and 7 days post-grafting (N=3 rats per time point). Axons emerged from the graft/lesion site by day 2 after grafting, and extended at a rapid rate of 1–2mm/day (Suppl. Fig. 4). The visualization of axon growth over time documents the extension of new axons and excludes the possible artifact that grafted cells fused with host neurons. Thus, axons extended in remarkably large numbers and over long distances, including extension through adult white matter. Indeed, time course studies indicated that initial axon outgrowth preferentially occurred through white matter (Suppl. Fig. 4).

Graft-derived axons in host white matter were frequently myelinated by host oligodendrocytes (i.e., cells myelinating graft-derived axons were not labeled for GFP; Fig. 3A–B). In addition, grafted cells that differentiated into neurons extended axons from the spinal cord lesion site into adjacent host ventral roots in every subject examined, with 6.8 ± 1.2 graft-derived axons quantified per 40μm-thick section of ventral root; Suppl. Fig. 2E–F). 56.7 ± 5.3% of these ventral root axons expressed the appropriate phenotypic motor neuronal marker choline acetyltransferase (ChAT; Suppl. Fig. 3F), likely derived from ChAT-expressing motor neurons inside grafts (Suppl. Fig. 2C). GFP-labeled axons were rarely detected in dorsal roots.

GFP-labeled, graft-derived axons in the host spinal cord formed dense bouton-like terminals around host dendrites and cell bodies, identified by labeling for the neuronal somal and dendritic markers MAP-2, the neuronal somal marker Tuj1 (βIII tubulin), and the motor neuron marker ChAT (Fig. 3C–E). Double immunofluorescent labeling for GFP and synaptophysin suggested synapse formation between grafted and host neurons in both rostral and caudal directions (Fig. 3E) at all distances from the lesion site, including sites sampled 25mm from the injury. Immunoelectron microscopy confirmed synapse formation between GFP-labeled graft-derived axons and host neurons and dendrites (Fig. 3F). Further, GFP-labeled terminal boutons expressed either the excitatory transmitter marker vesicular glutamate transporter 1/2 (vGlut1/2) or the inhibitory marker glutamic acid decarboxylase 65 (GAD65) (Fig. 3G–H). Many instances of co-localization of these terminal region markers with ChAT were also found (Fig. 3G–H). Collectively, these findings demonstrate exuberant projections of neural stem cell-derived axons from sites of spinal cord injury into the adult spinal cord together with synapse formation.

Neurons of the developing spinal cord express receptors to myelin-associated inhibitors such as Nogo (Josephson et al., 2002), a finding we confirmed in the present study in grafted tissue (Suppl. Fig. 5A). Thus, insensitivity to myelin-based inhibitors is an unlikely mechanism to account for the robust growth of axons observed in this study. Recently, the tumor suppressor gene “phosphatase and tensin homolog” (PTEN) has been identified as a major neuron-intrinsic regulator of axonal regeneration in the adult CNS (Park et al., 2008). PTEN inhibits the activity of “mammalian target of rapamycin” (mTOR), and neuronal knockout of PTEN has been reported to enhance central axonal regeneration (Park et al., 2008; Liu et al., 2010; Sun et al., 2011). To determine whether mTOR signaling is a mechanism contributing to the extensive growth of neural stem cell-derived axons through the lesioned adult CNS, we injected rapamycin, an mTOR inhibitor, into rats beginning two days after placement of grafts into the lesion site (6 mg/kg intraperitoneally, n=6 rats; 7

controls underwent vehicle injections). When examined two weeks later, rats subjected to mTOR blockade exhibited a significant, 50% reduction in graft-derived axonal outgrowth from the lesion compared to vehicle-injected controls ($P<0.05$; Fig. 4A; Suppl. Fig. 5B–E). Labeling for phospho-S6 (p-S6), an indicator of mTOR activity (Park et al., 2008), demonstrated abundant expression in graft-derived neurons and substantial reduction following rapamycin treatment (Suppl. Fig. 5H–J). Rapamycin injection did not alter neural stem cell graft survival or differentiation (Suppl. Fig. 5F–G, K). These findings demonstrate mTOR signaling as a mechanism contributing to the ability of early stage neurons to extend axons in the adult lesioned CNS.

Importantly, host axons also penetrated neural stem cell grafts in spinal cord lesion sites, including BDA-labeled reticulospinal axons and 5-HT labeled serotonergic (raphespinal) axons (Fig. 4B–G). Host inputs into grafts were both locally and supraspinally derived. While host supraspinal axons regenerated into grafts, in no case did they regenerate beyond the graft into host spinal cord parenchyma caudal to the lesion site. Like graft-derived axons, host axons penetrating grafts co-localized with the synaptic marker synaptophysin (Fig. 4F), establishing a mechanism for host-to-graft connectivity.

Functional and behavioral outcomes were measured in subjects that underwent T3 complete spinal cord transections and, two weeks later, neural stem cell implants in the lesion site (Fig. 5A). Hindlimb locomotion was severely impaired in both lesion control and grafted subjects for the first four weeks post-injury; in the 5^{th} week (three weeks post-grafting), recipients of neural stem cell grafts exhibited significant improvement on the BBB scale (Basso et al., 1996), reaching a functional plateau by the 8^{th} week post-lesion ($p<0.01$). The mean BBB score reached a level of 7, indicating movement about each joint of the hindlimb, in contrast to minimal movement if any in lesioned controls. To determine whether functional improvement depended on regeneration of host axons into the graft/lesion site, half the subjects underwent re-transection of the spinal cord just rostral to the T3 graft, resulting in a complete abolition of behavioral recovery when measured one week later (Fig. 5A and Suppl. Fig. 6).

To confirm the dependence of functional recovery on host axonal regeneration into the lesion site, electrophysiological measurements were made in 6 subjects. A stimulating electrode was placed in the dorsal C7 spinal cord (3 spinal segments above the lesion) and recordings were made at T6 (3 spinal segments below the lesion). In intact animals, stimulation at C7 evoked a short latency (3.42± 0.32 msec) response (Fig. 5B-i) that was entirely abolished by T3 complete transection (Fig. 5B-ii). In two-thirds of animals with neural stem cell grafts in the lesion site, evoked responses were restored (Fig. 5B-iii). Response latencies in the grafted group were prolonged (5.47 ± 0.24 msec compared to 3.42± 0.32 msec in intact subjects, $P<0.05$), suggesting formation of poly-synaptic relays through the graft. Response amplitudes in the grafted group (0.09 ± 0.03 mV) were smaller than intact subjects (0.27 ± 0.12 mV) ($P<0.05$; Fig. 5B-iii). Notably, re-transection of the spinal cord just rostral to the T3 graft completely abolished detectable activity upon C7 stimulation even when using high intensity stimuli (Fig. 5B-iv). To determine whether responses detected at T6 depended on the presence of synapses in the graft, the NMDA receptor blocker kynurenic acid (50 mM) was applied to the graft at T3, 7 weeks post-lesion. Kynurenic acid resulted in a significant, 50% reduction in the amplitude of the response recorded at T6 but did not affect latency of the response, indicating that excitatory synaptic transmission across the graft was required for detection of caudal transmission (Fig. 5C).

Thus, early stage neurons grafted in a fibrin matrix containing a growth factor cocktail extend large numbers of axons over long distances in the lesioned spinal cord, and form neuronal relays that significantly improve electrophysiological and functional outcomes.

The magnitude of functional effect substantially exceeds those previously reported in studies of fetal or stem cell grafts to the injured spinal cord, possibly due to enhanced graft survival generated by co-implantation with fibrin matrices containing growth factors. These results suggest strong translational possibilities. Accordingly, we repeated these studies using cultured *human* neural stem cells.

6 adult female athymic nude rats (T-cell deficient) underwent T3 complete transections. One week later, a suspension of neural stem cells derived from human fetal spinal cord (566RSCUBQT-GFP, see Methods; gift of NeuralStem, Inc.) was embedded into fibrin matrices containing a growth factor cocktail, as above. These cells are currently being used in a human clinical trial in amytrophic lateral sclerosis (Boulis et al., 2011). Function was assessed over the next 7 weeks in grafted animals and compared to six lesioned controls, then rats were sacrificed for anatomical studies. Grafts completely and consistently filled lesion cavities (Fig. 6A), and a majority of grafted cells (57±1.7%) expressed the mature neuronal marker NeuN (Fig. 6B). As in rat donor studies, remarkable numbers of axons emerged from the grafts and extended for very long distances, over a total of 17 spinal segments (Fig. 6C–E and Fig. 7). In the rostral direction, axons extended 25 mm above the lesion site to the C4 level (Fig. 7A–C), and in the caudal direction axons reached the upper lumbar spinal cord (Fig. 7D–F). GFP-labeled, graft-derived axons formed bouton-like terminals in the host gray matter and expressed human-specific synaptophysin (Fig. 6F), suggesting synaptic connectivity between grafted human and host rat neurons. Tumor formation by implanted human neurons was not observed within the lesion site or remotely in the host spinal cord. As observed in rat donor studies, grafts of human neural stem cells induced significant locomotor recovery after T3 complete transection (Fig. 6G), with movement about all joints of the lower extremities. Once again, re-transecting the spinal cord immediately rostral to the lesion site abolished hindlimb movement, indicating that functional recovery was dependent on inputs into the graft from the host.

To determine whether the ability to extend axons in vivo is a property expressed by stem cells derived from different human sources, we also tested the **H**arvard **U**niversity **E**mbryonic **S**tem cell **7** (HUES7) line (Cowan et al., 2004). HUES7 cells were neurally induced (Yuan et al., 2011) and embedded in the same growth factor cocktail-containing matrix, then grafted to sites of spinal cord injury (Suppl. Fig. 7); because this component of the study was purely anatomical, we used a C5 lateral spinal cord lesion (hemisection) in which animal care is less difficult. Once again, remarkable numbers of axons extended from the lesion over very long distances, reaching the brainstem in the rostral direction and the lumbar spinal cord caudally (Suppl. Fig. 7A–G). In gray matter, these human terminals abundantly expressed the pre-synaptic marker synaptophysin (Suppl. Fig. 7H).

DISCUSSION

Findings of the present study indicate that neural stem cells can specify sufficient information to permit extensive, long-distance central nervous system axonal regeneration; additional experimental manipulation of the inhibitory environment of the adult CNS is not required to achieve this long-distance regeneration. Moreover, the axon growth arising from neural stem cells can support functional improvement in the most severe model of spinal cord injury, complete spinal transection, when co-grafted in a supportive fibrin matrix containing a growth factor cocktail. Axons extend in large numbers and over remarkably long distances to form connections with host axons. Indeed, axons grew through white matter, gray matter, and into ventral roots, grew in high density, and elongated at a rapid rate of 1–2mm per day even through inhibitory white matter. Moreover, host supraspinal axons regenerated into the neural stem cell grafts. This reciprocal growth resulted in a five-point improvement on the BBB scale that reflects recovery of the ability to move all joints of the

hindlimbs. The mechanism of recovery, in contrast to previous studies with neural stem cells, is functional relay formation, indicated by the abolition of recovery by spinal re-transection immediately rostral to the lesion. These findings may accordingly represent the most comprehensive demonstration to date of the ability of novel neural relays to support functional recovery even after the most severe spinal cord injury (Steward et al., 2003).

Wictorin and colleagues reported in 1990 that early stage human fetal tissue grafted into partial striatal lesion sites could extend axons for long distances in the mature CNS (Wictorin et al., 1990). In 1997, Silver and colleagues also supported the concept that neurons could extend axons through adult CNS tissue over long distances, by grafting adult dorsal root ganglion neurons to white matter (Davies et al., 1997). However, these neurons did not extend axons across lesion sites and functional effects were not studied (Davies et al., 1999). More recently, Gaillard and colleagues reported long-distance extension of GFP-labeled axons from embryonic grafts placed into cortical lesion sites; this study was anatomical and lacked functional or circuit analysis (Gaillard et al., 2007). Fischer's group grafted mixed neuronal and glial restricted precursors to sites of partial spinal cord injury but reported only modest axonal outgrowth (Lepore and Fischer, 2005), and subsequent co-administration of growth factors enabled further axonal growth over only short distances of a few millimeters (Bonner et al., 2011). Previous studies of embryonic stem cell implants to sites of spinal cord injury used moderate and incomplete lesions, and reported only modest functional improvements (Cummings et al., 2005) (1–2 points on the BBB scale), with relatively modest graft survival in the lesion site. The classic embryonic spinal cord grafting literature (Jakeman and Reier, 1991; Theele et al., 1996; Giovanni et al 1997) used cells of a similar developmental stage to the rodent donor cells in the present study, but did not identify the extent to which early stage neurons were capable of extending very large numbers of axons over extraordinarily long distances in the lesioned adult nervous system; the improved survival, growth and outcomes in the present study are likely a result of the use of fibrin matrix and a growth factor cocktail, together with clear identification of cell fate and projection using the GFP reporter. Indeed, distances traversed by graft-derived axons in this study exceeded the length of the entire embryonic rat nervous system (Miller et al., 1998). Findings were not attributable to graft cell fusion with the host, as axons progressively elongated outward from the lesion over several days, an observation inconsistent with cell fusion.

Grafts of human neural stem cells exhibited growth that was equally extensive. Two different human cell sources, including 566RSC cells derived from human embryonic spinal cord (Johe et al., 1996) and HUES7 cells derived from human ES cells (Cowan et al., 2004; Yuan et al., 2011), exhibited identical patterns of growth in the injured adult spinal cord after neural induction. Thus, this growth potential is not cell-specific or species-specific, suggesting translational potential. Indeed, functional testing of 566RSC cells also revealed an ability to support extensive functional improvement in a severe SCI lesion.

Conclusion

We report an extensive number, distance and functional impact of axonal outgrowth from neural stem cell grafts, embedded in fibrin matrices containing growth factors, to sites of severe spinal cord injury. These findings indicate that properties intrinsic to the early stage neuron are sufficient to overcome barriers to growth in the adult CNS. There are important potential clinical implications: treatments were delayed for a clinically practical time frame of at least one week post-injury, resulted in significant functional improvement, and were achieved using a human neural stem source already employed in clinical trials for ALS (Boulis et al., 2011).

EXPERIMENTAL PROCEDURES

Animals

Adult female Fischer 344 rats (160–200 g, n=55) and athymic nude rats (T-cell deficient) (180–200 g, n=12) were subjects of this study. NIH guidelines for laboratory animal care and safety were strictly followed. Animals had free access to food and water throughout the study. All surgery was done under deep anesthesia using a combination (2 ml/kg) of ketamine (25 mg/ml), xylazine (1.3 gm/ml) and acepromazine (0.25 mg/ml).

Transplantation surgeries

Adult female Fischer 344 rats and athymic nude rats underwent T3 complete transection. A 2-mm-long block of spinal cord was cut and removed using a combination of iridectomy scissors and microaspiration, with visual verification to ensure complete transection ventrally and laterally. For rat-donor studies, grafting was performed two weeks after T3 transection. Embryonic day 14 (E14) spinal cords from transgenic Fischer 344-Tg (EGFP) rats, ubiquitously expressing GFP under the ubiquitin C promoter, provided donor tissue for grafting (Rat Resource and Research Center, University of Missouri, Columbia, Missouri). E14 spinal cord was dissected and dissociated according to the method of Harris et al. (2007). Dissociated E14 cells were re-suspended in a fibrin matrix (25 mg/ml fibrinogen and 25 U/ml thrombin, Sigma F6755 and T5772) containing growth factors to support graft survival (Willerth et al., 2007; Grumbles et al., 2009; Kadoya et al., 2009): BDNF (50 μg/ml, Peprotech, 452-02), neurotrophin-3 (NT-3; 50 μg/ml, Peprotech, 450-03), platelet-derived growth factor (PDGF-AA; 10 μg/ml, Sigma, P3076), insulin-like growth factor 1 (IGF-1; 10 μg/ml, Sigma, I8779), epidermal growth factor (EGF; 10 μg/ml, Sigma, E1257), basic fibroblast growth factor (bFGF; 10 μg/ml, Sigma, F0291), acidic fibroblast growth factor (aFGF; 10 μg/ml, Sigma, F5542), glial cell line-derived neurotrophic factor (GDNF; 10 μg/ml, Sigma, G1401), hepatocyte growth factor (HGF; 10 μg/ml, Sigma, H9661), and calpain inhibitor (MDL28170, 50 μM, Sigma, M6690). The graft mixture was microinjected into the lesion cavity as a 10μl cell suspension and subjects survived another 7 weeks (n=26). Animals underwent functional testing, electrophysiological assessment and anatomical analysis and were compared to 6 lesion-only controls. To identify molecular mechanisms underlying axonal outgrowth from donor cells, 13 additional subjects underwent lesions and rat neural stem cell grafts, then received either rapamycin (LC Laboratories, 6 mg/kg of 20 mg/ml solution; n=6 animals) or vehicle (n=7) intraperitoneally every other day starting two days post-grafting, as previously described (Park et al., 2008). Animals survived an additional two weeks. An additional 12 subjects underwent lesion and grafts, and were perfused 1, 2, 3 or 7 days after transplantation (n=3 per time point) to examine the time course of axonal outgrowth from the lesion site. Two weeks before perfusion, reticulospinal tract axons were anterogradely labeled by injection of 0.5μl of 10% biotinylated dextran amine (BDA; MW 10,000, Molecular Probes) into each of four sites spanning both the right and left gigantocellular reticular nucleus (bregma, 11–12.5 mm; lateral, 8 mm; depth, 8.2–7.3 mm) (Jin et al., 2002).

For human neural stem cell donor studies, cultured human fetal spinal cord NSCs (NSI-566RSC), were provided by NeuralStem, Inc. Methods for procuring cells have been published previously (Johe et al., 1996; Boulis et al., 2011). Briefly, the cervical and upper thoracic region of an 8-week human fetal spinal cord was dissociated and suspended by trituration in serum-free, modified N2 medium containing 100 mg/l human plasma apo-transferrin, 25mg/l recombinant human insulin, 1.56g/l glucose, 20nM progesterone, 100μM putrescine, and 30nM sodium selenite in DMEM/F12. 10ng/ml FGF2 was added as a mitogen and cells were serially expanded as monolayer cultures in T175 flasks or 150mm plates coated with 100μg/ml poly-D-lysine (Johe et al., 1996). FGF2 was added every two

days, and cells were first passaged on day 16. Cells were harvested at each subsequent passage upon reaching 75% confluence and were stored in liquid nitrogen. They were not retained after passage 20. For shipping, cells were thawed one day prior to grafting, washed and shipped overnight to UC San Diego at 2–8°C. Viability exceeded 80% the next day. Cells expressed GFP under the ubiquitin C promoter, enabling in vivo tracking of cell survival, differentiation and process outgrowth. Cells were implanted into spinal cord lesion sites one week after T3 complete transection (N=6 animals) and were compared to lesioned, ungrafted controls (N=6). Animals survived for 7 weeks and underwent functional testing, as described above. We also grafted a second human stem cell source. Proliferating HUES7 colonies were cultured on mouse fibroblasts and induced to form embryoid bodies. During the nestin-positive stage the rosettes were removed, single cell suspensions prepared, and the $CD184^{+}/CD271^{-}/CD44^{-}/CD24^{+}$ population of hES-NSCs were FAC-sorted and expanded in the presence of FGF-2 (Yuan et al., 2011). Cells were embedded in fibrin matrices containing growth factors as described above, and were grafted into sites of C5 hemisection in adult female athymic (nude) rats (N=6). Comparison was made to lesioned, ungrafted controls (N=6). Animals survived for 3 months and were sacrificed for anatomical studies, as described above. This was a purely anatomical study; functional outcomes were not examined.

Histology and immunohistochemistry

Animals were perfused with 4% paraformaldehyde in 0.1 M phosphate buffer (pH 7.2). Spinal cords were dissected, post-fixed overnight at 4°C and then transferred to 30% sucrose for 72 hours. 1.5 cm-long horizontal sections of spinal cords containing the lesion/graft site were sectioned on a cryostat set at 30μm thickness. Coronal sections from the spinal cord, rostral and caudal to the T3 lesion/transplant site, were examined. Immunohistochemistry was performed to assess survival, maturation, integration and outgrowth of grafted neurons as previously described (Lu et al., 2003). Free-floating sections were incubated with primary antibodies against jellyfish green fluorescent protein (GFP; rabbit, Invitrogen @ 1:1,500 or goat from Chemicon @ 1:1500 to label GFP-expressing neural stem cells); GFAP (mouse from Chemicon @ 1:1500 or rabbit from Dako at @ 1:1500 to label astrocytes); NeuN (mouse from Chemicon @ 1:200 to label mature neurons); choline acetyltransferase (ChAT; goat from Chemicon @ 1:200 to label spinal cord motor neurons and motor axons); MAP-2 (mouse from Chemicon @ 1:10,000 to label mature neurons); ßIII tubulin (mouse from Chemicon @ 1:500 to label immature and mature neurons), neurofilament (NF; mouse from Chemicon @ 1:1500 to label axons); serotonin (5-HT; polyclonal antibody from Immunostar @ 1:20,000 to label raphespinal axons); myelin-associated glycoprotein (MAG; mouse from Chemicon @ 1:200 to label myelin); glutamic acid decarboxylase 65 or 67 (GAD65, goat from RD System, or GAD67, mouse from Millipore @1:1000 to label gabaergic neurons/terminals); vesicular glutamate transporters 1/2 (vGlut1/2, mouse from Chemicon @1:1000 to label glutamatergic terminals); synaptophysin (mouse from Chemicon @ 1:1000 to label presynaptic terminals), Adenomatous Ployposis Coli (APC, monoclonal antibody from Oncogene @ 1:400 to label oligodendrocytes), phospho-S6 kinase (p-S6, rabbit from Cell Signaling Technology @ 1:200 to label ribosomal protein S6 phosphorylated at serine 235 and 236). Sections were incubated overnight at 4°C, then incubated in Alexa 488, 594 or 647 conjugated goat or donkey secondary antibodies (1:250, Invitrogen) for 2.5 hr at room temperature. For nuclear staining, 4&,6-diamidino-2-phenylindole (DAPI) (200 ng/ml) was added to the final wash. BDA-labeled reticulospinal tract axons were detected by double fluorescent labeling with GFP. After blocking with 5% donkey serum, every 6^{th} section was incubated with primary antibody directed against GFP (rabbit) and Alexa 594-conjugated streptavidin (to bind to BDA-labeled reticulospinal tract axons) overnight at 4°C. After washes, sections were incubated with Alexa 488 conjugated donkey anti-rabbit secondary antibodies for 2.5 hr at room temperature.

For examination and quantification of GFP-labeled axons, light level GFP immunolabeling was performed in every sixth section incubated overnight at 4^0C with GFP primary antibody (rabbit at 1:3000) and then with horseradish peroxidase (HRP) conjugated secondary antibodies (1:50, Vector Laboratory, Burlingame, CA) for 1 hr at room temperature. Diaminobenzidine (0.05%) with nickel chloride (0.04%) were used as chromagens, with reactions sustained for 10 min at room temperature.

Quantification of neural cell density and axon number

Cellular differentiation was determined by counting individual cells labeled for NeuN, GFAP or APC within a fixed box size of 1600 × 1200 pixels at 400× magnification within the graft, divided by the total number of cells per sample box labeled with DAPI. Two randomly selected fields corresponding to the graft epicenter were counted in each subject for each label, and all analyses were conducted in a blinded manner. An average of 170, 150 and 92 NeuN-, APC- and GFAP-labeled cells were counted in each of six grafted animals, respectively, and divided by the mean number of DAPI-labeled nuclei in the sampled field (a mean of 586 DAPI-labeled nuclei/field). The number of GFP-labeled axons emerging from a typical graft placed at the T3 transection site was quantified using StereoInvestigator (MicroBrightField, mbfbioscience.com) as previously described (Rosenzweig et al., 2010). Briefly, in every 6^{th} sagittal section, a dorsoventral line was drawn 500 μm caudal to the graft/host interface under 40× magnification. The tissue was then examined under 600× magnification, and GFP-labeled axons that intersected this line were marked and counted. The sampling fraction was 8.3%. In addition, GFP axon number was quantified in every 6^{th} section both rostral and caudal to the graft to study molecular mechanisms of axonal growth after rapamycin treatment. Lesion margins were determined using GFAP and GFP double fluorescent immunolabeling, and axons crossing a vertical line in horizontal sections 1, 3, and 5 mm rostral and caudal to the lesion/graft border were counted at 200× magnification. Total axon number/subject was estimated by multiplying by the sampling fraction. Observers were blinded to group identity in all surgical and quantitative procedures.

Semi-quantative RT-PCR

For RT-PCR of NgR1, 500 ng total RNA from E14, P1 or adult spinal cord was used as the template in a 20 ul reaction with random hexamer priming using the Superscript III kit (Invitrogen). 1 ul RT product was used in standard PCR with different cycle numbers. PCR primers: 1)/\ GAPDH:/\ TGGAGTCTACTGGCGTCTT,/\ TGTCATATTTCTCGTGGTTCA; 2) NgR1: AAGAGGGCGTCCTCCGG, CGGCATGACTGGAAGCT.

Electron microscopy

Electron microscopic analysis of synapse formation and myelination was performed according to the methods of Knott et al. (2009). Briefly, two rats with T3 complete transections that received rat neural stem cell grafts were perfused with 4% paraformaldehyde plus 0.25% glutaraldehyde (survival time three months), and spinal cord parenchyma 2mm caudal to the lesion/graft site was sectioned in the coronal plane, then immunolabeled for GFP with Diaminobenzidine (DAB) and nickel chloride. Sections were then post-fixed with 1% osmium tetroxide, dehydrated, embedded in Durcupan resin, and sectioned at 60 nm thickness. Individual GFP-labeled axons or axonal terminals were located and assessed using a FEI 200KV Sphera microscope at the UCSD CryoElectron Microscopy Facility.

Electrophysiology

Descending transmission of electrical activity through grafts was assessed using previously described techniques (Bradbury et al., 2002). In brief, a bipolar stimulating electrode, consisting of a pair of 85 μm tungsten microelectrodes (0.5 MOhm, WPI, Inc.) spaced 1 mm apart, was lowered 300–500 μm into the cord at the C7 spinal segment. Brief (0.1 msec) square wave pulses were delivered at 3–5 second intervals and responses were averaged over 40 trials. Field responses were recorded using a 1 mm diameter silver ball electrode placed (i) at T6, three segments caudal to the graft (see Fig. 6b). Confirmation of electrical transmission through the graft was confirmed by re-transecting the cord immediately above the graft, and by applying kynurenic acid (50 mM in ACSF) to the graft at the T3 segment.

Functional analysis

The BBB open field 21-point locomotion rating scale (Basso et al., 1996) was assessed weekly by two independent observers blinded to group identity.

Statistical Analysis

In all quantification procedures and behavioral analyses, observers were blinded to the nature of the experimental manipulation. Multiple group comparisons were made using one-way analysis of variance (ANOVA; JMP software) at a designated significance level of 95%. Two-group comparisons were tested by Student's t-test. Data are presented as mean ± SEM.

Supplementary Material

Refer to Web version on PubMed Central for supplementary material.

Acknowledgments

We thank Dr. Ramsey Samara for electrophysiological assistance; Janet Weber, Andrea Chan and Jeffrey Kwan for technical assistance; the Rat Resource and Research Center, University of Missouri, Columbia, Missouri, for providing GFP rats; and Dr. Farquhar for use of the electron microscopy core facility. Human neural stem cells were a gift from NeuralStem, Inc. This work was supported by the Veterans Administration, NIH (NS09881), Canadian Spinal Research Organization, The Craig H. Neilsen Foundation, and the Bernard and Anne Spitzer Charitable Trust.

REFERENCES

Bamber NI, Li H, Aebischer P, Xu XM. Fetal spinal cord tissue in miniguidance channels promotes longitudinal axonal growth after grafting into hemisected adult rat spinal cords. Neural Plast. 1999; 6:103–121. [PubMed: 10714264]

Baska KM, Manandhar G, Feng D, Agca Y, Tengowski MW, Sutovsky M, Yi YJ, Sutovsky P. Mechanism of extracellular ubiquitination in the mammalian epididymis. J Cell Physiol. 2008; 215:684–696. [PubMed: 18064599]

Basso DM, Beattie MS, Bresnahan JC. Graded histological and locomotor outcomes after spinal cord contusion using the NYU weight-drop device versus transection. Exp Neurol. 1996; 139:244–256. [PubMed: 8654527]

Bonner JF, Connors TM, Silverman WF, Kowalski DP, Lemay MA, Fischer I. Grafted neural progenitors integrate and restore synaptic connectivity across the injured spinal cord. J Neurosci. 2011; 31:4675–4686. [PubMed: 21430166]

Boulis NM, Federici T, Glass JD, Lunn JS, Sakowski SA, Feldman EL. Translational stem cell therapy for amyotrophic lateral sclerosis. Nat Rev Neurol. 2011; 8:172–176. [PubMed: 22158518]

Bradbury EJ, Moon LD, Popat RJ, King VR, Bennett GS, Patel PN, Fawcett JW, McMahon SB. Chondroitinase ABC promotes functional recovery after spinal cord injury. Nature. 2002; 416:636–640. [PubMed: 11948352]

Bregman BS, McAtee M, Dai HN, Kuhn PL. Neurotrophic factors increase axonal growth after spinal cord injury and transplantation in the adult rat. Exp Neurol. 1997; 148:475–494. [PubMed: 9417827]

Bryda EC, Pearson M, Agca Y, Bauer BA. Method for detection and identification of multiple chromosomal integration sites in transgenic animals created with lentivirus. Biotechniques. 2006; 41:715–719. [PubMed: 17191616]

Buchli AD, Schwab ME. Inhibition of Nogo: a key strategy to increase regeneration, plasticity and functional recovery of the lesioned central nervous system. Ann Med. 2005; 37:556–567. [PubMed: 16338758]

Cowan CA, Klimanskaya I, McMahon J, Atienza J, Witmyer J, Zucker JP, Wang S, Morton CC, McMahon AP, Powers D, et al. Derivation of embryonic stem-cell lines from human blastocysts. N Engl J Med. 2004; 350:1353–1356. [PubMed: 14999088]

Cummings BJ, Uchida N, Tamaki SJ, Salazar DL, Hooshmand M, Summers R, Gage FH, Anderson AJ. Human neural stem cells differentiate and promote locomotor recovery in spinal cord-injured mice. Proc Natl Acad Sci U S A. 2005; 102:14069–14074. [PubMed: 16172374]

David S, Aguayo AJ. Axonal elongation into peripheral nervous system “bridges” after central nervous system injury in adult rats. Science. 1981; 214:931–933. [PubMed: 6171034]

Davies SJ, Fitch MT, Memberg SP, Hall AK, Raisman G, Silver J. Regeneration of adult axons in white matter tracts of the central nervous system. Nature. 1997; 390:680–683. [PubMed: 9414159]

Davies SJ, Goucher DR, Doller C, Silver J. Robust regeneration of adult sensory axons in degenerating white matter of the adult rat spinal cord. J Neurosci. 1999; 19:5810–5822. [PubMed: 10407022]

Fawcett JW. Overcoming inhibition in the damaged spinal cord. J Neurotrauma. 2006; 23:371–383. [PubMed: 16629623]

Filbin MT. Recapitulate development to promote axonal regeneration: good or bad approach? Philos Trans R Soc Lond B Biol Sci. 2006; 361:1565–1574. [PubMed: 16939975]

Fitch MT, Silver J. CNS injury, glial scars, and inflammation: Inhibitory extracellular matrices and regeneration failure. Exp. Neurol. 2008; 209:294–301. [PubMed: 17617407]

Gaillard A, Prestoz L, Dumartin B, Cantereau A, Morel F, Roger M, Jaber M. Reestablishment of damaged adult motor pathways by grafted embryonic cortical neurons. Nat Neurosci. 2007; 10:1294–1299. [PubMed: 17828256]

Giovanini MA, Reier PJ, Eskin TA, Wirth E, Anderson DK. Characteristics of human fetal spinal cord grafts in the adult rat spinal cord: influences of lesion and grafting conditions. Exp Neurol. 1997; 148:523–543. [PubMed: 9417830]

Grumbles RM, Sesodia S, Wood PM, Thomas CK. Neurotrophic factors improve motoneuron survival and function of muscle reinnervated by embryonic neurons. J Neuropathol Exp Neurol. 2009; 68:736–746. [PubMed: 19535998]

Harris J, Lee H, Tu CT, Cribbs D, Cotman C, Jeon NL. Preparing e18 cortical rat neurons for compartmentalization in a microfluidic device. J Vis Exp. 2007:305. [PubMed: 18989412]

He Z, Koprivica V. The Nogo signaling pathway for regeneration block. Annu Rev Neurosci. 2004; 27:341–368. [PubMed: 15217336]

Houle JD, Tom VJ, Mayes D, Wagoner G, Phillips N, Silver J. Combining an autologous peripheral nervous system “bridge” and matrix modification by chondroitinase allows robust, functional regeneration beyond a hemisection lesion of the adult rat spinal cord. J. Neurosci. 2006; 26:7405–7415. [PubMed: 16837588]

Jakeman LB, Reier PJ. Axonal projections between fetal spinal cord transplants and the adult rat spinal cord: a neuroanatomical tracing study of local interactions. J Comp Neurol. 1991; 307:311–334. [PubMed: 1713233]

Jin Y, Fischer I, Tessler A, Houle JD. Transplants of fibroblasts genetically modified to express BDNF promote axonal regeneration from supraspinal neurons following chronic spinal cord injury. Exp Neurol. 2002; 177:265–275. [PubMed: 12429228]

Johe KK, Hazel TG, Muller T, Dugich-Djordjevic MM, McKay RD. Single factors direct the differentiation of stem cells from the fetal and adult central nervous system. Genes Dev. 1996; 10:3129–3140. [PubMed: 8985182]

Josephson A, Trifunovski A, Widmer HR, Widenfalk J, Olson L, Spenger C. Nogo-receptor gene activity: cellular localization and developmental regulation of mRNA in mice and humans. J Comp Neurol. 2002; 453:292–304. [PubMed: 12378589]

Kadoya K, Tsukada S, Lu P, Coppola G, Geschwind D, Filbin MT, Blesch A, Tuszynski MH. Combined intrinsic and extrinsic neuronal mechanisms facilitate bridging axonal regeneration one year after spinal cord injury. Neuron. 2009; 64:165–172. [PubMed: 19874785]

Knott GW, Holtmaat A, Trachtenberg JT, Svoboda K, Welker E. A protocol for preparing GFP-labeled neurons previously imaged in vivo and in slice preparations for light and electron microscopic analysis. Nat Protoc. 2009; 4:1145–1156. [PubMed: 19617886]

Lepore AC, Fischer I. Lineage-restricted neural precursors survive, migrate, and differentiate following transplantation into the injured adult spinal cord. Exp Neurol. 2005; 194:230–42. [PubMed: 15899260]

Liu K, Lu Y, Lee JK, Samara R, Willenberg R, Sears-Kraxberger I, Tedeschi A, Park KK, Jin D, Cai B, et al. PTEN deletion enhances the regenerative ability of adult corticospinal neurons. Nat Neurosci. 13:1075–1081. [PubMed: 20694004]

Lu P, Jones LL, Snyder EY, Tuszynski MH. Neural stem cells constitutively secrete neurotrophic factors and promote extensive host axonal growth after spinal cord injury. Exp Neurol. 2003; 181:115–129. [PubMed: 12781986]

Mayer-Proschel M, Kalyani AJ, Mujtaba T, Rao MS. Isolation of lineage-restricted neuronal precursors from multipotent neuroepithelial stem cells. Neuron. 1997; 19:773–85. [PubMed: 9354325]

Miller KE, Douglas VD, Richards AB, Chandler MJ, Foreman RD. Propriospinal neurons in the C1-C2 spinal segments project to the L5-S1 segments of the rat spinal cord. Brain Res Bull. 1998; 47:43–47. [PubMed: 9766388]

Park KK, Liu K, Hu Y, Smith PD, Wang C, Cai B, Xu B, Connolly L, Kramvis I, Sahin M, et al. Promoting axon regeneration in the adult CNS by modulation of the PTEN/mTOR pathway. Science. 2008; 322:963–966. [PubMed: 18988856]

Rosenzweig ES, Courtine G, Jindrich DL, Brock JH, Ferguson AR, Strand SC, Nout YS, Roy RR, Miller DM, Beattie MS, et al. Extensive spontaneous plasticity of corticospinal projections after primate spinal cord injury. Nat Neurosci. 13:1505–1510. [PubMed: 21076427]

Steward O, Zheng B, Tessier-Lavigne M. False resurrections: distinguishing regenerated from spared axons in the injured central nervous system. J Comp Neurol. 2003; 459:1–8. [PubMed: 12629662]

Sun F, Park KK, Belin S, Wang D, Lu T, Chen G, Zhang K, Yeung C, Feng G, Yankner BA, et al. Sustained axon regeneration induced by co-deletion of PTEN and SOCS3. Nature. 480:372–375. [PubMed: 22056987]

Theele DP, Schrimsher GW, Reier PJ. Comparison of the growth and fate of fetal spinal iso- and allografts in the adult rat injured spinal cord. Exp Neurol. 1996; 142:128–143. [PubMed: 8912904]

Tuszynski, MH.; Lu, P. Axon plasticity and regeneration in injured spinal cord. In: Kordower, JH.; Tuszynski, MH., editors. CNS Regeneration, Basic Science and Clinical Advances. Second Edition. Vol. Chapter 13. Academic Press; 2008. p. 319-335.

Wictorin K, Brundin P, Gustavii B, Lindvall O, Bjorklund A. Reformation of long axon pathways in adult rat central nervous system by human forebrain neuroblasts. Nature. 1990; 347:556–558. [PubMed: 1699131]

Willerth SM, Faxel TE, Gottlieb DI, Sakiyama-Elbert SE. The effects of soluble growth factors on embryonic stem cell differentiation inside of fibrin scaffolds. Stem Cells. 2007; 25:2235–2244. [PubMed: 17585170]

Yuan SH, Martin J, Elia J, Flippin J, Paramban RI, Hefferan MP, Vidal JG, Mu Y, Killian RL, Israel MA, et al. Cell-surface marker signatures for the isolation of neural stem cells, glia and neurons derived from human pluripotent stem cells. PLoS One. 2011; 6:e17540. [PubMed: 21407814]

Highlights

- Neural stem cells grow axons over very long distances after severe spinal cord injury
- New synaptic relays are formed, improving electrophysiological and functional outcome
- Rodent and human neural stem cells exhibit similar growth properties
- Mechanisms intrinsic to early stage neurons overcome adult nervous system inhibition

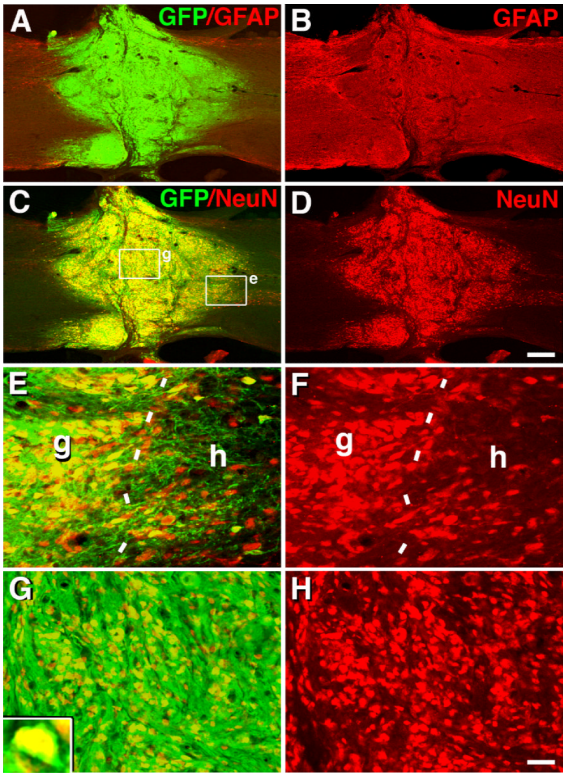

Figure 1. Survival, Filling and Differentiation of Neural Stem Cell Grafts in T3 Complete Transection Site

(A–B) Overview of **GFP** and **GFAP** fluorescent immunolabeling in a horizontal section demonstrates excellent graft survival, integration and filling of T3 complete transection site, seven weeks post-grafting. **(C–D) GFP** and **NeuN** labeling confirm extensive neuronal differentiation/maturation of grafted rat neural stem cells. (**E–F**) Higher magnification from **c** showing excellent integration and transition from host (**h**) neurons to grafted (**g**) neurons (dashed lines) (**E: GFP, NeuN; F, NeuN** alone). **(G–H)** Higher magnification from center of graft showing high density of NeuN-labeled neurons (inset) (**G: GFP, NeuN; H, NeuN** alone). Scale bar: A–D, 320 μm; E–H, 48 μm. Also see Figure S1 and S2.

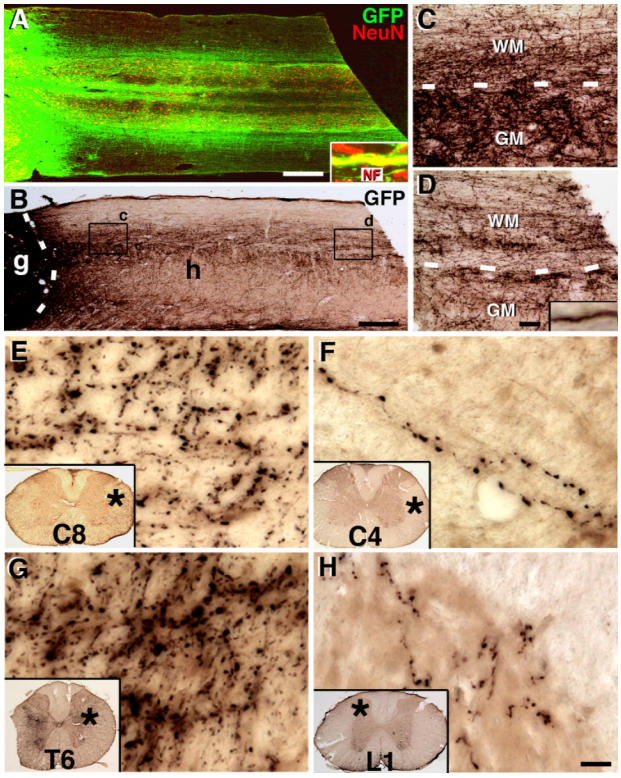

Figure 2. Extensive Long-Distance Axonal Outgrowth from Neural Stem Cell Grafts

(**A**) **GFP** and **NeuN** immunolabeling reveals that **GFP**-expressing neural stem cell grafts robustly extend axons into the host spinal cord rostral and caudal to the T3 complete transection site (caudal shown) over the 12mm length of the horizontal section. Extensive regions of the host spinal cord contain graft-derived projections in white matter and gray matter. Inset shows that **GFP**-labeled projections arising from grafts express neurofilament (**NF**), confirming their identity as axons. (**B**) Light-level GFP immunolabeling also clearly reveals the density and distribution of axons extending from the lesion site. Boxes are shown at higher magnification in C, D. (**C**) Dense numbers of GFP-labeled axons are present in host white matter (WM) and gray matter (GM) 2mm caudal to the lesion, and (**D**) large numbers of axons remain at the end of the block of tissue, 6mm caudal to the lesion. (**E**) A high density of GFP-labeled axons is present in the lateral portion of C8, three spinal segments above the lesion, and (**F**) remain detectable at C4, 7 spinal segments above the lesion. Asterisk indicates locations of higher magnification view. (**G**) GFP-labeled axons also extend in dense numbers caudally to T6 white matter and gray matter (shown) and (**H**) caudally to L1. Overall, axons extend at least 25 mm in each direction. Scale bar: A–B, 600 μm; B–C, 40 μm; D–G, 10 μm. Also see Figure S3 and S4.

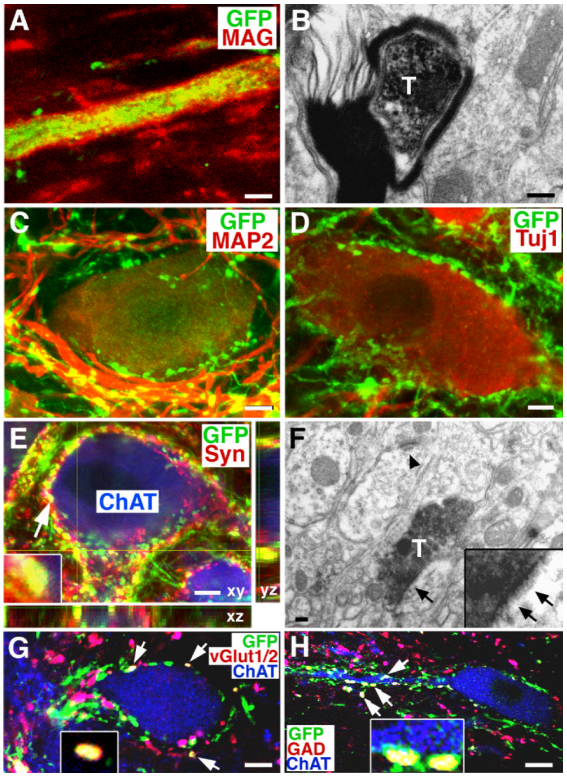

Figure 3. Myelination, Synapse Formation and Expression of Neurotransmitters

(A–B) Graft-derived, **GFP**-labeled axons are myelinated in many cases, (**red**, myelin-associated glycoprotein, **MAG**, confirmed by electron microscopy (T, transplanted, GFP-labeled axon). **(C) GFP**-expressing axon terminals are closely associated with host **MAP-2**-expressing neurons and dendrites, and **(D)** host **Tuj1**-expressing neuronal somata. **(E)** A z-stack image triple labeled for **GFP**, synaptophysin (**Syn**, inset), and **ChAT**, indicating co-association of graft-derived axons with a synaptic marker in direct association with host motor neurons (arrowhead indicates one of several examples). **(F)** Electron microscopy confirms that DAB-labeled **GFP**-expressing axon terminals form synapses (arrows) with host dendrites. Arrowhead indicates a separate, host-host synapse. **(G–H)** Expression of **vGlut1/2** or **GAD65** by **GFP**-labeled axons (arrows and insets) in close association with host motor (**ChAT**-labeled) neurons. Scale bar: A, 3μm; B, 200nm; C–E, 8μm; F, 200nm; G, 7μm; H, 6μm.

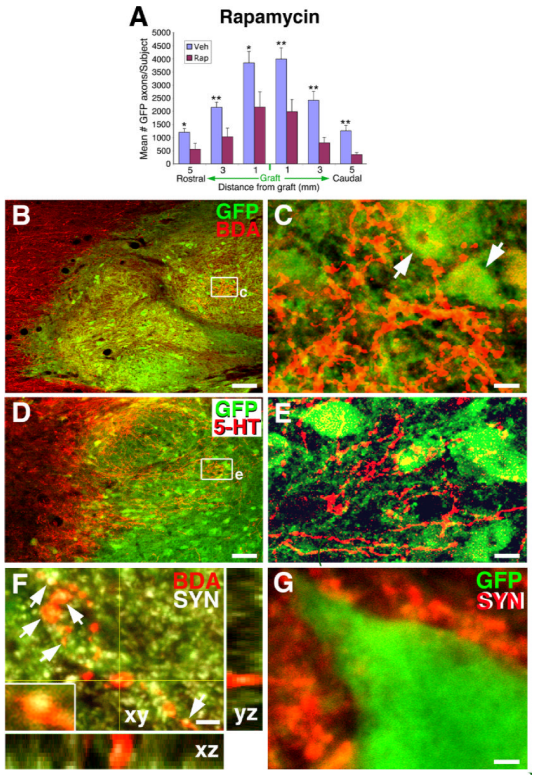

Figure 4. Rapamycin Reduces Axon Growth; Host Axons Innervate Grafts

(A) Treatment with the mTOR inhibitor rapamycin significantly reduced outgrowth of graft-derived axons (*p<0.05, **p<0.01; see also Suppl. Fig 5). Veh, vehicle; Rap, rapamycin treated. Data are represented as mean ± SEM. **(B–C)** Host reticulospinal axons labeled with **BDA** regenerate into **GFP**-expressing neural stem cell grafts in site of T3 complete transection (**C**, from boxed area of panel **B**; arrows indicate **GFP**-labeled grafted cells with neuronal morphology). (**D–E**) Host serotonergic axons immunolabeled for **5-HT** regenerate into **GFP** expressing E14 neural stem cell grafts in lesion site. (**F**) Bouton-like structures on host reticulospinal axons regenerating into graft co-localize with synaptophysin in a Z-stack image (arrows). (**G**) Host synaptophysin terminals (**red**) are closely apposed to **GFP**-labeled grafted cells exhibiting neuronal morphology. Scale bar: B, 64μm; C, 12μm; D, 70 μm; E, 10 μm; F–G, 2μm. .

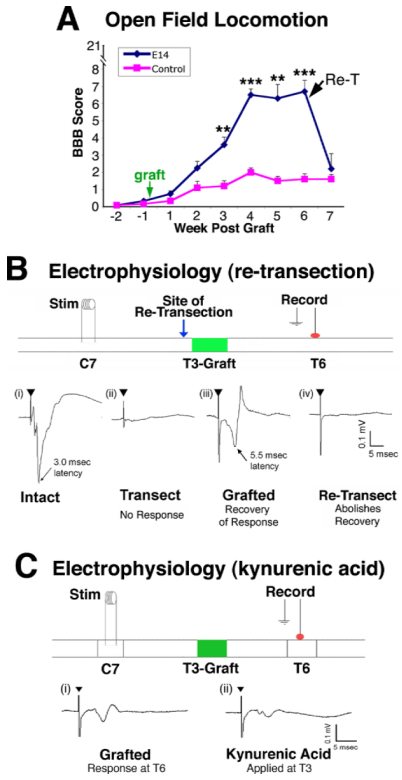

Figure 5. Functional and Electrophysiological Improvement after T3 Complete Transection

(A) Hindlimb locomotion: BBB scores after T3 complete transection show significant improvement in subjects that received neural stem cell grafts (NSC, n=6) compared to lesioned controls (n=6). Re-transection (arrow, Re-T) at rostral interface of graft with host abolishes functional improvements when assessed one week later (**p<0.01, ***p<0.001). Data are represented as mean ± SEM. **(B)** Electrophysiological transmission across the T3 complete lesion site: (i) In intact animals, stimulation at C7 evoked a short latency (~3.0 msec), large amplitude response at T6. (ii) Transection of the cord at T3 completely abolished this response. (iii) In 4 of 6 lesion/grafted animals, recovery of an evoked response of prolonged latency (~5.5 msec) was observed. (iv) Re-transection of the spinal cord at T3, just rostral to the graft (green arrow), abolished the recovered evoked response. **(C)** Kynurenic acid (50 mM), a blocker of excitatory synapses, was applied to the graft to determine whether excitatory transmission across synapses in the graft was required to detect responses at T6. Indeed, kynurenic acid application substantially reduced the amplitude but not the latency of the evoked response. Also see Figure S6.

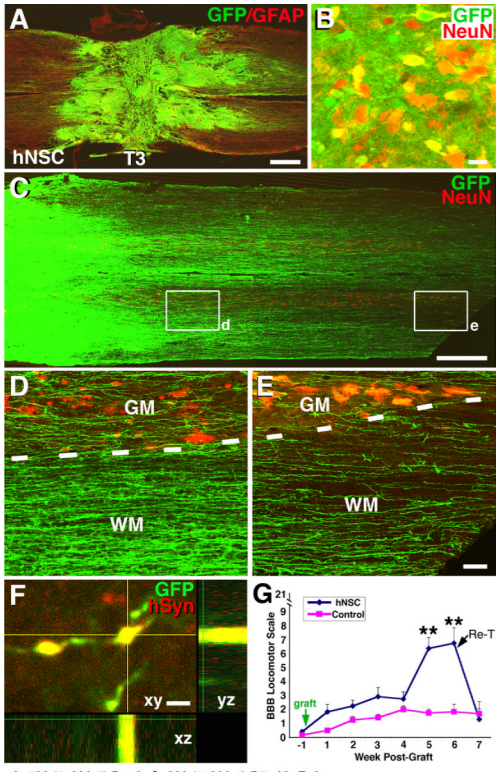

Figure 6. Human Neural Stem Cell Grafts in Fibrin Matrices after T3 Transection: Long-Distance Axonal Growth, Connectivity and Functional Improvement

(**A**) **GFP**-expressing 566RSC human neural stem cells (NSCs) survive and completely fill T3 complete transection site, 7 weeks post-grafting (**GFP**, green; **GFAP**, red). (**B**) **GFP** and **NeuN** labeling reveals that many grafted human neural stem cells express mature neuronal markers. Field is from graft center. **(C–E)GFP**-expressing human neurons robustly extend axons into the host spinal cord caudal and rostral to the complete T3 transection site (caudal shown). Axons extend through both white matter (WM) and gray matter (GM). (**F**) **GFP**-labeled human axon terminals express human-specific synaptophysin (**hSyn**) in host gray matter. Site shown is 7 mm caudal to lesion. Scale bar: A, 500 μm; B, 10 μm; C, 600 μm; D–E, 60 μm; F 3 μm. **(G)** There is significant functional improvement after human NSC grafts to sites of T3 complete transection (**p<0.01). Re-transection (arrow, Re-T) at rostral interface of graft completely abolishes functional recovery assessed one week later, indicating that host inputs are required to improve function. Data are represented as mean ± SEM.

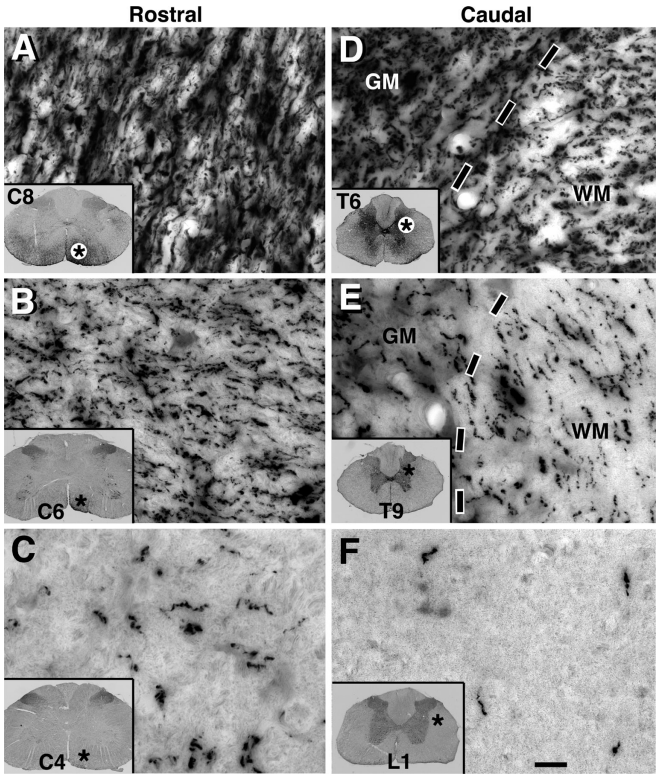

Figure 7. Dense Axonal Outgrowth from Implants of Human 566RSC Neural Stem Cells

(A) Very large numbers of GFP-labeled axons extend into host spinal cord rostral to T3 transection site, 7 weeks post-grafting. C8 segment shown. **(B–C)** GFP-labeled axons are present in C6 and C4 white matter, five and seven spinal segments above the lesion, respectively. Asterisks indicate location of higher magnification views. (**D–F**) GFP-labeled axons also extend in high density caudal to T6 and T9, and are present in both white matter (WM) and gray matter (GM, dashed lines indicate interface). (**F**) Axons continue to extend caudally to L1. Overall, axons extend at least 25 mm in each direction in all subjects. Scale bar: 15 μm.